Published in final edited form as:
*J Mol Biol*. 2014 January 23; 426(2): 412–422. doi:10.1016/j.jmb.2013.10.002.

# The Structure of Xis reveals the basis for Filament Formation and insight into DNA bending within a mycobacteriophage Intasome

**Shweta Singh**[1], **Joseph G. Plaks**[1], **Nicholas J. Homa**[1,4], **Christopher G. Amrich**[1], **Annie Heroux**[2], **Graham F. Hatfull**[1], and **Andrew P. VanDemark**[1,3]

[1]Department of Biological Sciences, University of Pittsburgh, Pittsburgh PA 15260, USA

[2]Department of Biology, Brookhaven National Laboratory, Upton, NY 11973, USA

## Abstract

The Recombination Directionality Factor, Xis, is a DNA bending protein that determines the outcome of integrase-mediated site-specific recombination by redesign of higher-order protein-DNA architectures. Although the attachment site DNA of Mycobacteriophage Pukovnik is likely to contain four sites for Xis binding, Xis crystals contain five subunits in the asymmetric unit, four of which align into a Xis filament, and a fifth that is generated by an unusual domain swap. Extensive intersubunit contacts stabilize a bent filament-like arrangement with Xis monomers aligned head-to-tail. The structure implies a DNA bend of ~120°, which is in agreement with DNA bending measured *in vitro*. Formation of *attR*-containing intasomes requires only Int and Xis, distinguishing Pukovnik from lambda. Therefore, we conclude that in Pukovnik, Xis-induced DNA bending is sufficient to promote intramolecular Int-mediated bridges during intasome formation.

### Keywords

DNA recombination; mycobacteriophage Pukovnik; Xis; DNA bending; filament; structure

## Introduction

Prophage establishment by temperate bacteriophages typically involves integrase-mediated site-specific recombination between the phage *attP* and chromosomal *attB* site [1]. Of the large family of phage-encoded integrases of the tyrosine recombinase type that mediate these events, phage lambda represents a well-studied prototype [1; 2; 3]. In lambda, integration requires integrase (Int), the host integration factor (IHF), a large (250 bp) *attP* site that contains both core-type and arm-type integrase binding sites, and a smaller *attB* site (25 bp). Strand exchange occurs within the shared common core sequence and proceeds through a



[3]Corresponding Authors **Contact Information** 4249 Fifth Ave, 360A Langley Hall, University of Pittsburgh, Pittsburgh PA 15260 andyv@pitt.edu, phone: (412) 648-0110, fax: (412) 624-4759.
[4]Present address: 426 CARL building, Duke University, Durham, NC, 27710, njh16@duke



**Accession Codes.** Coordinates and structure factors for Pukovnik Xis have been deposited at the Protein Data Band under accession number 4J2N.

Holliday Junction (HJ) intermediate [4; 5]. Prophage excision, which occurs during induction of lytic growth, is also catalyzed by Int, requires IHF, but is strongly dependent on the Recombination Directionality Factor (RDF), Xis [6; 7]. These Int-mediated reactions are strongly directional. In the absence of Xis, the only productive pair of substrates are *attP* and *attB*, whereas in the presence of Xis, only *attL* and *attR* recombine; Xis is also a strong inhibitor of integrative recombination [3].

The molecular basis of this directionality lies in the requirement for the formation of higher-order protein-DNA architectures for synapsis and strand exchange to occur [6]. Int is a bivalent DNA binding protein that can bind simultaneously to core- and arm-type binding sites forming intra- or inter-molecular protein bridges [8]. Formation of recombinationally-active complexes requires the introduction of DNA bends, and this is accomplished through the binding of IHF [9; 10] to the H1, H2 and H' site in lambda *attP*, and the binding of Xis to the X1, X', and X2 binding sites in *attP* (and *attR*) [6; 11; 12]. The 72-residue Lambda Xis bends DNA upon binding, and also contributes cooperative interactions through the binding of its extreme C-terminus to the arm-type binding N-terminal domain of Int[13; 14; 15]. Structural analysis of lambda Xis shows that it binds DNA through a winged-helix motif of the MerR superfamily, using contacts between a central loop and the wing motif to mediate interactions between Xis proteins when bound to DNA and presumably drive cooperative binding and the formation of a micronucleoprotein filament with a modest bend [16; 17].

Mycobacteriophage L5 encodes a far distant relative of lambda Int, but shares many common features [18]. Its *attP* site contains arm- and core-type integrase binding sites, although the specific arrangements of arm-type sites is different than in lambda *attP* [19]. L5 also requires a host factor for both integration and excision although this mycobacterial Integration Host Factor (mIHF) is unrelated at the sequence level to *E. coli* IHF and only binds specifically to *attP* in the presence of L5 Int [20; 21]. The L5 Xis (gp36) is a far distant relative of Lambda Xis [22; 23], but is also small (56 aa), and binds to four sites (X1-X4) within *attR* to promote formation of an *attR* intasome in which Int forms protein bridges between the core-type sites and the P1/P2 arm-type sites [24]. It is not known if there are direct interactions between L5 Xis and L5 Int, but L5 Xis lacks the C-terminal domain that contributes this function to Lambda Xis.

Phage discovery and genomics has generated a large collection of sequenced mycobacteriophages that can be grouped into clusters and subclusters according to their overall nucleotide sequence similarities [25; 26]. Phage L5 lies within Subcluster A2 along with seven other closely related phages, six of which also encode tyrosine integrases [27]. All of these contain an *attP* core closely related to L5 *attP* and are predicted to integrate into the same *attB* site [28]. However, the sequence similarity outside of the core is generally much lower, suggesting differences in the specificities of other components of the recombination reactions. Pukovnik is one such phage.

Here we describe the structure of Pukovnik Xis, in which there are five subunits in the asymmetric unit, four of which are aligned for binding to the four Xis binding sites in Pukovnik *attR*, but one of which is formed entirely by a domain-swap interaction. Xis monomers pack together via multiple cooperative interactions to form a filament with left-handed superhelical twist with a bending angle of 120°.This high degree of bending is in agreement with DNA bending observed in vitro, suggesting the filament is consistent with Xis-DNA architecture within an *attR* containing intasome. We observe that *attR* intasomes can be formed by Int and Xis alone, bypassing the requirement for IHF found in other systems. We predict that the extensive interactions formed in Pukovnik Xis filaments stabilize a highly bent DNA conformation that facilitates the simultaneous binding of integrase to both core and arm-type binding sites within *attR*.

## Results

### Pukovnik Xis is required for prophage excision

Mycobacteriophage Pukovnik is a relative of phage L5, and both are grouped in Subcluster A2 [29]. They share interrupted segments of nucleotide sequence similarity that together span 66% of the genome and range from 65% to 85% nucleotide identity. Pukovnik and L5 contain closely related *attP* common core sequences indicating they use the same *attB* site for integration (Fig. S1), and the integrases share 81% amino acid sequence identity. The organizations of Pukovnik and L5 *attP* sites are similar with two pairs of arm-type Int binding sites (P1 and P2, P4 and P5) flanking the core, and a lone site (P3) between P2 and the core; in L5, P3 is not required for either integration or excision and its role is not known [19; 24]. In L5, the host factor mIHF binds between the core and P4, but only forms stable protein-DNA complexes in the presence of L5 Int [20]. There are predicted to be four Xis binding sites (X1 – X4) between P2 and P3 and are similarly positioned in L5 and Pukovnik (Fig. S1). Pukovnik Xis binds cooperatively to *attR* DNA (see Fig. 5) but with reduced cooperativity to a smaller (50 bp) fragment containing the X1-X4 sites (Fig. 1B), as also reported for Lambda Xis [16]. Binding is specific to the X1-X4 binding sequences as an altered X1-X4 sequence does not support significant binding (Fig. 1B, S1). Pukovnik Xis stimulates integrase-mediated excision (Fig. 1C) and inhibits integration as reported previously for L5 [22; 24]. Pukovnik Int by itself does not form electrophoretically stable complexes with *attR* DNA, but addition of Xis results in generation of a new complex (Fig. 1D). This is reminiscent of protein binding to *attR* in the L5 system, in which Int alone fails to form a complex with *attR*, but when both Xis and mIHF are added, an *attR* intasome is formed in which Int is presumed to form a bridge between the core and arm-type sites. Although the Pukovnik system differs in that formation of the *attR*-Int-Xis complex is mIHF-independent (Fig. 1D, E), it seems likely that it also includes a similar bridging interaction, and a complex – an *attR* intasome – with overall similarity to the L5

### Structure of the Pukovnik Xis

The structure of Pukovnik Xis was determined by X-ray crystallography. Phasing was accomplished using the SAD method from crystals containing selenomethionine-substituted protein and refined against native data at 2.35 Å resolution to a free R value of 26.7% (see Material and Methods and Table I for a complete description of the structure determination process and statistics). The asymmetric unit contains five individual Xis subunits which stack onto each other through an extensive array of protein-protein interactions forming a filament with left-handed superhelical twist (Fig. 2A & B). Stacking within the filament is quite regular with each monomer exhibiting a ~60° bending angle as well as a twist of 40°. Within the asymmetric unit, four Xis protomers are contained within the filament region with the fifth protomer being positioned adjacent to the filament and participating in stacking with a symmetry-related filament. All protomers adopt a compact winged-helix fold with very little structural variation between them (0.3 Å r.m.s.d over all Cα atoms). Crystallization required the inclusion of either ammonium sulfate or ammonium phosphate, many of which were well resolved particularly in the domain-swap interface (Fig. S2). Despite limited sequence identity, Pukovnik Xis is also highly similar structurally to other Xis proteins currently described in the structural database, including phage λ Xis (1LX8) (1.9 Å r.m.s.d over 42 Cα atoms) [173031]. The domain-swap Xis pair are formed by a dramatic rearrangement within the loop connecting β1 and β2 (residues 36-39) allowing the C-terminal residues 40-56 to interact with the N-terminal 35 residues of a neighboring Xis monomer, reforming two Xis monomers (Fig. S2). The resulting domain-swap Xis proteins retain the canonical fold but are linked together by their wing regions.

## Subunit interactions as well as direct DNA contacts promote excision

While the overall fold of Pukovnik gp37 is similar to other Xis proteins, there are few sequence motifs that are conserved between lambda and mycobacteriophage Xis proteins from the A2 subcluster of mycobacteriophages (Fig. 3A). We therefore sought to determine sequence elements responsible for DNA recognition. We began this exploration by generating a mutant with substitutions at positions K19, R22, and N23 within the DNA recognition helix and with substitutions at R34 and R38 within the wing, positions that mediate direct contacts with DNA in lambda [16; 32]. These putative DNA recognition mutants were purified and tested for their ability to recognize *attR* X1-X4 DNA and as predicted all show a strong reduction in the affinity for *attR* DNA (Fig. S3). We conclude that Pukovnik and Lambda Xis proteins recognize DNA similarly.

We next sought to determine if the protein-protein interactions that are mediating filament formation within our structure are also important for DNA recognition and phage excision. These contacts are features that differentiate Pukovnik and λ Xis. The most important of these are residues 51-54 of Pukovnik Xis, which make extensive contacts with the wing of the adjacent monomer. These contacts include several backbone hydrogen bonds, forming a three stranded beta sheet with the Wing of an adjacent subunit (Fig. 3B). This interaction provides a platform for cooperative interactions positioning Xis subunits in a head-to-tail arrangement that drives filament formation. Deletion of the C-terminal tail through the introduction of a stop codon after residue 50 greatly diminishes DNA binding affinity and abolishes excision (Fig. 3C & 3D). Structures of lambda Xis (residues 1-55) in complex with DNA [16], indicate that the equivalent tail sequences make only minimal contacts between protein subunits, with subunit-subunit contacts being driven primarily by electrostatic interactions between acidic residues in the wing (D37 and E40) and basic residues on the adjacent subunit (R14, R16, and K49). We note however, the Lambda Xis protein used for X-ray structure determination lacks the C-terminal 17 residues that are involved in Xis – Int interactions [15], and although this region is not required for cooperative Xis binding [17], the deletion could influence the position of the extreme C-terminus in the X-ray structure. In Pukovnik, this interaction surface is maintained as an additional contact that drives filament formation, with L35 from the wing engaging the neighboring subunit through numerous hydrophobic interactions (Fig. 3B). A L35A substitution interferes with cooperative binding to *attR* DNA (Fig. 3C), indicating that the ability to form a Xis filament is impaired even in the presence of the C-terminal tail. Surprisingly, the L35A substitution is still capable of supporting excision (Fig. 3D), suggesting that the intersubunit interactions provided by the C-terminal tail are sufficient to support a functionally viable conformation even when DNA binding affinity is diminished. Taken together these results demonstrate that DNA binding of Pukovnik Xis is mediated by direct interactions with the Wing and DNA recognition helixes as expected but is also facilitated by an extensive series of interactions that drive filament formation and thereby provide the physical basis for the cooperativity observed in Xis binding.

## Formation of attR intasomes

Since formation of *attR* intasomes in Pukovnik does not require mIHF, we predicted that formation of this higher order structure would be strongly dependent on Xis filament formation. To test this, we examined the ability of various Xis mutants to form an *attR* intasomes, in the presence of Int (Fig. 4). In this assay, we find that Int alone is incapable of binding *attR*, however the addition of small concentrations of Xis (14.6 nM) stimulates the formation of a higher-order Int-Xis-DNA complex (Fig. 4). Xis mutants incapable of binding a 365 bp *attR* fragment (Δ51-56, K19A/R22A/N23A, and R34A/R38A) are inactive in *attR* intasome formation (Fig. 4), although a L35A mutant, which affects contacts between Xis monomers, displays diminished capacity to stimulate *attR* intasome formation.

Together these data are consistent with the interpretation that both direct DNA binding interactions intersubunit interactions promote filament formation that stabilize the *attR* intasome in a cooperative manner.

### The Xis filament and its implications for DNA bending

DNA architecture within the synaptic complex is a critical feature that distinguishes the ability of integrase to promote integrative or excision recombination. The arrangement of Xis subunits observed within the filament segment of our crystal implies that Xis imparts a substantial bend upon binding to DNA. From the stacking of subunits within the filament (Fig. 2B), we estimate this bend to be approximately 120°, or about 30° for each subunit, assuming that all four sites are occupied. We note that three protomers of lambda Xis exert an overall bend of 72° [16] – in agreement with the 45-90° estimated from λ Xis-DNA complex mobility studies [12] – or about 24° per protomer. The extent of DNA bending introduced is thus similar for the Pukovnik and λ Xis proteins – consistent with the overall DNA contact patterns being similar – although the overall degree of bending in Pukovnik *attR* is greater than in λ *attR* because of the greater number of bound protomers.

To ascertain the extent to which *Pukovnik* Xis facilitates DNA bending, we inserted Xis binding sites X1-X4 into the plasmid pBend2 [33]. Digestion of this plasmid with various restriction enzymes releases linear fragments of equal size containing the Xis binding cassette at different positions within the fragment (Fig. 5). Xis complexes formed with these DNA fragments were analyzed by native PAGE and the relative differences in mobility observed between a centrally or terminally located binding cassette was used to calculate the degree of DNA bending (Fig. 5) [33]. Using this system we observed an overall bend of 106.4 ± 3.0 degrees, in good agreement with the 120° predicted from the structural studies.

## Discussion

Bacteriophage tyrosine integrase-mediated site-specific recombination events present excellent models for understanding regulation of biological processes through modulation of higher order macromolecular architectures. Moreover, the huge genetic diversity of the phage population provides a plethora of informative variations providing mechanistic insights. The structural and molecular analysis of the Pukovnik Xis described here presents a new view of how DNA binding and bending can modulate the action of a tyrosine integrase in the absence of host factor.

Although the Pukovnik and lambda Xis proteins adopt a similar overall fold with similar DNA contacts, there are many functional distinctions between them. First, the lambda Xis protein is longer than Pukovnik Xis (and other closely related Xis proteins) due to an extended C-terminal tail. The C-terminal 17 residues of lambda Xis and the related HK022 Xis are poorly defined in NMR analyses [17; 30], and are excluded from the crystallographic analysis [16]. The extreme C-terminus of Pukovnik Xis is, however, critical for interaction with adjacent Xis protomers within filament-like structures, and is thus required for normal Xis function.

A second difference is in the unusual domain-swap interaction in the Pukovnik Xis filament for which there is no counterpart in lambda Xis. Although structures for three other functionally related proteins have been described [HK022 [30], transposon Tn*916* [31] and the prophage excise TorI [34]], all of these were determined by NMR spectroscopy in the absence of DNA, and neither filament-like organizations nor domain-swaps are apparent.

Lastly, we generated a model of a DNA-bound Pukovnik Xis filament to examine the constraints such a filament might place on intasome architecture. To do this, we removed the

domain swap protomer that bridges filaments within the crystal (residues 1-35 of the yellow subunit and 36-56 of the cyan subunit in Fig. 2B), noting that the remaining swapped protomer is nearly identical to the canonical fold (Fig. S2B). We then modeled DNA onto the Pukovnik filament through superposition of individual Pukovnik protomers with the structure of a lambda Xis-DNA complex (PDB 2IEF, chain B). In the resulting model, the *attR* DNA sequence leading towards core sequence C is separated from the beginning of the X1 site by ~75 Å (Fig. 6A). The model indicates that bending is not constrained within a plane as was observed for the IHF-DNA complex [35], or the lambda Xis-DNA complex [16], but instead is twisted out of the plane by ~60°. We compared our model, with the structure of the lambda Xis-DNA complex (PDBid 2IEF, containing Xis proteins bound at X1, X1.5, and X2 positions) via superposition of Xis proteins at the X1 site (Fig. 6B). The resulting model clearly suggests that Xis binding places a different set of constraints on DNA architecture than in lambda. As stated previously, this model of the Pukovnik nucleoprotein filament predicts a 120° bend in the DNA which is close to the 106° bend we observe *in vitro*, however at ~30° of bend per monomer, our *in vitro* results suggest that 3.5 monomers are binding per *attR* DNA fragment. The difference in bending angle could suggest that four Xis monomers bind but that some degree of relaxation within the DNA bound filament is not described in this simple model. Alternatively, it could suggest that only three Xis proteins are binding. This is supported by the observation that there is somewhat lower sequence conservation between L5 and Pukovnik *attR* DNA sequences at their X1 sites (Fig. S1C). Our data cannot distinguish between these possibilities.

The substantial differences in DNA bending between Pukovnik and lambda may be result of the need to perform excision from *attR* sites with different organizations (Fig. S4). For example, we note that there are two IHF binding sites within Lambda *attR*. In contrast, Pukovnik *attR* does not contain IHF binding sites. Finally, in lambda *attR* there are only three Xis binding site ($X_1$, $X_{1.5}$, and $X_2$) rather than the four Xis binding sites in Pukovnik and related phages. The overall distances between the core sites and the outermost arm-type binding site (110-120 bp) are similar in lambda and Pukovnik *attR*, and we presume that similar DNA bending is required to form Int-mediated intramolecular bridges. However, Lambda accomplishes this through the combined action of Xis and IHF, whereas Pukovnik does this by Xis alone.

An attractive scenario explaining the evolutionary relationships of the Lambda and Pukovnik integration systems is one in which the Pukovnik system is more similar to the ancestral state from which Lambda was derived. For example, loss of one of the Xis binding sites from the precursor state could have arisen through the acquisition of FIS binding sites that provide dependence on FIS at low Xis concentrations [36; 37]. The reduction in Xis-associated DNA bending might have provided the selective pressure for the gain of IHF binding sites.

## Material and Methods

### Plasmids and DNA substrates

Plasmid pMH57 (pattB) has been described [38]. DNA fragments (546 bp) containing *attP* site was amplified from the Pukovnik genomic DNA and cloned into the *Eco*R1 and *Bam*H1 site of the pUC19 plasmid to obtain pSS19. DNA fragments of 490 bp and 345 bp containing *attL* and *attR* were amplified by PCR from the product of *in vitro* integration (between pMH57 and pSS19) reactions and cloned into the *Hind*III and *Nde*1 site of pMOS Blue to obtain pSS21 and pSS22, respectively.

### Preparation of radiolabeled DNA

The digestion of plasmid pSS21 with *Hind*III and *Nde*1 generated a 490 bp DNA fragment containing the *attL* site. A 365 bp DNA fragment containing the *attR* site was generated by PCR amplification from the plasmid pSS22. These DNA fragments containing the *attL* (490 bp) and *attR* (365 bp) site were gel extracted and labeled by end-labeling with T4 polynucleotide kinase.

### *In vitro* recombination assay

*In vitro* integrative recombination was carried out between pSS19 (*attP*) and pMH57 (*attB*) in a recombination buffer containing 20mM Tris (pH-7.5), 25mM NaCl, 10mM EDTA, 10mM Spermidine and 1mM DTT in final volume of 10μl. Wherever needed, pMH57 was cut by *Sca*1 to make linear *attB* substrate for reactions. Reactions using super coiled or linear double stranded *attB* DNA containing 0.03pmol of pMH57 and super coiled *attP* DNA added in ratio indicated in each experiment.

*In vitro* excision assays were performed between pSS21 (*attL*) and pSS22 (*attR*) in a recombination buffer containing 10mM Tris (pH-7.5), 25mM NaCl, 5mM EDTA, 10mM Spermidine, 1mM DTT and 0.2mg/ml BSA in final volume of 10μl. Wherever needed, pSS21was cut by *Sca*1 to make linear *attL* substrate for reactions. Reactions using super coiled or linear double stranded *attL* DNA containing pSS21 and super coiled *attR* DNA added in indicated ratio.

Both the integration and excision reaction were incubated at 37°C for up to 4h and product were treated with 1mg/ml proteinase K and 0.5% of SDS at 60°C for 10-15 min. The products were separated on 0.8% agarose gel in 1x TBE running buffer and visualized by ethidium bromide staining.

### DNA-binding assays

Approximately 4ng of labeled DNA was incubated with the indicated amounts of Int, mIHF and Xis (wild-type and mutants) in a buffer containing 10mM Tris (pH-7.5), 25mM NaCl, 5mM EDTA, 10mM Spermidine, 1mM DTT, 0.2mg/ml BSA and 1μg Calf Thymus DNA, in a total volume of 10μl. The reactions were incubated at 37°C for one hour and the protein-DNA complexes were separated from the free DNA on a non-denaturing 4% (unless otherwise stated) polyacrylamide gel at 4°C.

### Xis purification

The complete coding sequence for mycobacteriophage Pukovnik excise (Xis) was PCR amplified from isolated genomic DNA and inserted into the bacterial expression vector pLC3 (a kind gift of Dr. Jim Sacchettini) using tradition cloning techniques. The resulting plasmid coded for an N-terminal $His_6$-MBP fusion tag which is removable via digestion with TEV protease, leaving the sequence GDITH attached to the N-terminus of the protein. The $His_6$-MBP-Xis protein was expressed using ZY autoinduction media[39] and the bacterial strain BL21 DE3 Codon-Plus (RIPL). Cells were harvested by centrifugation and lysed in 25 mM Tris pH 8.0, 500 mM NaCl, 10% glycerol, 5 mM Imidazole, 1 mM β-mercaptoethanol, plus protease inhibitors. Lysate was cleared by centrifugation at 30,000 × g, and Xis was purified by nickel affinity chromatography using Ni-NTA resin (Qiagen). The $His_6$-MBP-tag was removed via overnight digestion with TEV protease digestion, followed by a second round of nickel affinity chromatography to remove TEV and other contaminants. The resulting sample was further purified using cation exchange chromatography and peak fractions were subjected to gel filtration using a Sephacryl S-200 (GE Healthcare). Purified Xis was then dialyzed into 100 mM NaCl, 10 mM Hepes pH 7.5, and 1 mM β-

mercaptoethanol and concentrated to ~25 mg/mL using a Vivaspin concentrator (Millipore) prior to crystallization trials. Final protein purity was >99% as verified by SDS-PAGE. Selenomethionine Xis was expressed using PASM media [39], and the purification was similar to the native protein with addition of 5 mM β-mercaptoethanol in all the buffers. The final selenomethionine Xis protein concentration was 20.4 mg/mL in 25 mM NaCl and 10 mM Hepes pH 7.5.

### Xis Mutants

To enhance the yield of Xis protein, the coding sequence for Xis was amplified and cloned into the bacterial expression vector pMCSG7 (which contains a TEV cleavable N-terminal polyhistidine tag but no MBP tag) via ligation independent cloning. Single, double, and triple amino acid mutations were introduced into Xis using the QuickChange protocol (Stratagene) utilizing pMCSG7-Xis plasmid as a template. The Δ51-56 C-terminal truncation was also cloned into the pMCSG7 vector as with the wild-type. Expression and purification of the Xis mutants were performed in a similar manner as wild type.

### Integrase and Integration Host Factor Purification

The coding regions for Pukovnik integrase (pInt) and *Mycobacterium smegmatis* integration host factor (mIHF) were PCR amplified and cloned into pMCSG7 to express N-terminal His-tagged fusions cleavable by TEV protease. IHF was expressed using ZY autoinduction media as with Xis while pInt was expressed via IPTG induction in LB. Both proteins were purified using nickel and heparin affinity chromatography, and protein purity was judge at >99% by SDS-PAGE.

### Xis crystallization and structure determination

Crystals were initially obtained using the sitting drop vapor diffusion method at 20 °C against a reservoir solution containing 0.2 M ammonium sulfate and 20% polyethylene glycol 3350. Single crystals measuring approximately 0.2 × 0.2 × 0.05 mm form over the period of two weeks from drops containing 0.8 μL of protein and 1.0 μL of well solution (100 mM ammonium sulfate and 13.5% PEG 3350). Crystals were cryoprotected by a stepwise transition into well solution supplemental with 30% MPD and 15% PEG 3350. Selenomethionine crystals were grown in the same manner.

Crystals of Pukovnik Xis belong to space group $C222_1$ with $a$=89.5, $b$=130.5, and $c$=92.2 Å. Diffraction data from crystals of selenomethionine substituted Xis were collected at beamline X25 at the National Synchrotron Light Source. Integration, scaling, and merging of diffraction data was performed using HKL2000 [40]. Phases were determined experimentally via single-wavelength anomalous dispersion (SAD) using crystals containing selenomethionine substituted protein. Phases were calculated using the AutoSOL routine within PHENIX [41] and a starting model built into the resulting electron density. This initial model was then refined against native data collected in house using a FR-E rotating anode with VariMax optics and a Saturn944 CCD detector. The integration, scaling and merging of diffraction data was performed using HKL2000. The initial model was refined within PHENIX using positional refinement, simulated annealing, isotropic B-factor refinement, and TLS refinement. Model quality was analyzed using MolProbity [42] and the final model contains no Ramachandran outliers.

### Permutation Assay

DNA sequence containing the Xis binding cassette (sites X1-X4) from Pukovnik *attR* was inserted into the pBend2 plasmid[43]. Digesting the resulting plasmid with EcoRV, MluI, or the other indicated restriction enzymes resulted in DNA fragments of equal length but with

X1-X4 either centrally or terminally located. Complexes of these oligonucleotides with Xis were formed with 25 ng of the indicated DNA fragment, using 0.25 μM Xis and separated by native gel electrophoresis. The location of Xis-DNA complexes were determined by staining with SybrGreen and mobilities for the various DNA fragments were measured directly using ImageJ software. The DNA bending angle was determined by the equation $\mu_M/\mu_E = \cos(\alpha/2)$ where $\mu_M/\mu_E$ is the relative mobility of the centrally bound to the terminally bound oligonucleotide and $\alpha$ is the angle of DNA bending [33].

## Supplementary Material

Refer to Web version on PubMed Central for supplementary material.

## Acknowledgments

We thank M. Schmidt and J. Sacchettini for sharing resources and helpful advice. This work was supported by National Institutes of Health grant AI59114 to G.F.H. J.P and N.H. were supported by a Science Education Grant from the Howard Hughes Medical Institutes to the University of Pittsburgh.

## Abbreviations

| | |
|---|---|
| **Int** | Integrase |
| **IHF** | Integration Host factor |

## References

1. Landy A. Dynamic, structural, and regulatory aspects of lambda site-specific recombination. Annu Rev Biochem. 1989; 58:913–49. [PubMed: 2528323]
2. Van Duyne GD. Lambda integrase: armed for recombination. Curr Biol. 2005; 15:R658–60. [PubMed: 16139195]
3. Azaro, MA.; Landy, A. λ Int and the λ Int family. In: Craig, NL.; Craigie, R.; Gellert, M.; Lambowitz, AM., editors. Mobile DNA II. American Society Microbiology; Washington, D.C.: 2002. p. 118-148.
4. Franz B, Landy A. The Holliday junction intermediates of lambda integrative and excisive recombination respond differently to the bending proteins integration host factor and excisionase. Embo J. 1995; 14:397–406. [PubMed: 7835349]
5. Nunes-Duby SE, Azaro MA, Landy A. Swapping DNA strands and sensing homology without branch migration in lambda site-specific recombination. Curr Biol. 1995; 5:139–48. [PubMed: 7743177]
6. Kim S, Landy A. Lambda Int protein bridges between higher order complexes at two distant chromosomal loci attL and attR. Science. 1992; 256:198–203. [PubMed: 1533056]
7. Bushman W, Yin S, Thio LL, Landy A. Determinants of directionality in lambda site-specific recombination. Cell. 1984; 39:699–706. [PubMed: 6239693]
8. Moitoso de Vargas L, Kim S, Landy A. DNA looping generated by DNA bending protein IHF and the two domains of lambda integrase. Science. 1989; 244:1457–61. [PubMed: 2544029]
9. Ellenberger T, Landy A. A good turn for DNA: the structure of integration host factor bound to DNA. Structure. 1997; 5:153–7. [PubMed: 9032076]
10. Robertson CA, Nash HA. Bending of the bacteriophage lambda attachment site by Escherichia coli integration host factor. J Biol Chem. 1988; 263:3554–7. [PubMed: 2831189]
11. Kim S, Moitoso de Vargas L, Nunes-Duby SE, Landy A. Mapping of a higher order protein-DNA complex: two kinds of long-range interactions in lambda attL. Cell. 1990; 63:773–81. [PubMed: 2146029]

12. Thompson JF, Landy A. Empirical estimation of protein-induced DNA bending angles: applications to lambda site-specific recombination complexes. Nucleic Acids Res. 1988; 16:9687–705. [PubMed: 2972993]

13. Numrych TE, Gumport RI, Gardner JF. Characterization of the bacteriophage lambda excisionase (Xis) protein: the C-terminus is required for Xis-integrase cooperativity but not for DNA binding. Embo J. 1992; 11:3797–806. [PubMed: 1396573]

14. Wu Z, Gumport RI, Gardner JF. Defining the structural and functional roles of the carboxyl region of the bacteriophage lambda excisionase (Xis) protein. J Mol Biol. 1998; 281:651–61. [PubMed: 9710537]

15. Cho EH, Gumport RI, Gardner JF. Interactions between integrase and excisionase in the phage lambda excisive nucleoprotein complex. J Bacteriol. 2002; 184:5200–3. [PubMed: 12193639]

16. Abbani MA, Papagiannis CV, Sam MD, Cascio D, Johnson RC, Clubb RT. Structure of the cooperative Xis-DNA complex reveals a micronucleoprotein filament that regulates phage lambda intasome assembly. Proc Natl Acad Sci U S A. 2007; 104:2109–14. [PubMed: 17287355]

17. Sam MD, Papagiannis CV, Connolly KM, Corselli L, Iwahara J, Lee J, Phillips M, Wojciak JM, Johnson RC, Clubb RT. Regulation of directionality in bacteriophage lambda site-specific recombination: structure of the Xis protein. J Mol Biol. 2002; 324:791–805. [PubMed: 12460578]

18. Lee MH, Hatfull GF. Mycobacteriophage L5 integrase-mediated site-specific integration in vitro. J Bacteriol. 1993; 175:6836–41. [PubMed: 8226625]

19. Peña CE, Lee MH, Pedulla ML, Hatfull GF. Characterization of the mycobacteriophage L5 attachment site, attP. J Mol Biol. 1997; 266:76–92. [PubMed: 9054972]

20. Pedulla ML, Lee MH, Lever DC, Hatfull GF. A novel host factor for integration of mycobacteriophage L5. Proc Natl Acad Sci U S A. 1996; 93:15411–6. [PubMed: 8986825]

21. Pena CE, Kahlenberg JM, Hatfull GF. Assembly and activation of site-specific recombination complexes. Proc Natl Acad Sci U S A. 2000; 97:7760–5. [PubMed: 10869430]

22. Lewis JA, Hatfull GF. Identification and characterization of mycobacteriophage L5 excisionase. Mol Microbiol. 2000; 35:350–60. [PubMed: 10652095]

23. Lewis JA, Hatfull GF. Control of directionality in integrase-mediated recombination: examination of recombination directionality factors (RDFs) including Xis and Cox proteins. Nucleic Acids Res. 2001; 29:2205–16. [PubMed: 11376138]

24. Lewis JA, Hatfull GF. Control of Directionality in L5 Integrase-mediated Site-specific Recombination. J Mol Biol. 2003; 326:805–21. [PubMed: 12581642]

25. Hatfull GF. Complete Genome Sequences of 138 Mycobacteriophages. J Virol. 2012; 86:2382–2384. [PubMed: 22282335]

26. Hatfull GF, Pedulla ML, Jacobs-Sera D, Cichon PM, Foley A, Ford ME, Gonda RM, Houtz JM, Hryckowian AJ, Kelchner VA, Namburi S, Pajcini KV, Popovich MG, Schleicher DT, Simanek BZ, Smith AL, Zdanowicz GM, Kumar V, Peebles CL, Jacobs WR Jr. Lawrence JG, Hendrix RW. Exploring the mycobacteriophage metaproteome: phage genomics as an educational platform. PLoS Genet. 2006; 2:e92. [PubMed: 16789831]

27. Hatfull GF. The secret lives of mycobacteriophages. Adv Virus Res. 2012; 82:179–288. [PubMed: 22420855]

28. Peña CE, Stoner JE, Hatfull GF. Positions of strand exchange in mycobacteriophage L5 integration and characterization of the attB site. J Bacteriol. 1996; 178:5533–6. [PubMed: 8808947]

29. Hatfull GF, Jacobs-Sera D, Lawrence JG, Pope WH, Russell DA, Ko CC, Weber RJ, Patel MC, Germane KL, Edgar RH, Hoyte NN, Bowman CA, Tantoco AT, Paladin EC, Myers MS, Smith AL, Grace MS, Pham TT, O'Brien MB, Vogelsberger AM, Hryckowian AJ, Wynalek JL, Donis-Keller H, Bogel MW, Peebles CL, Cresawn SG, Hendrix RW. Comparative Genomic Analysis of 60 Mycobacteriophage Genomes: Genome Clustering, Gene Acquisition, and Gene Size. J Mol Biol. 2010; 397:119–143. [PubMed: 20064525]

30. Rogov VV, Lucke C, Muresanu L, Wienk H, Kleinhaus I, Werner K, Lohr F, Pristovsek P, Ruterjans H. Solution structure and stability of the full-length excisionase from bacteriophage HK022. Eur J Biochem. 2003; 270:4846–58. [PubMed: 14653811]

31. Abbani M, Iwahara M, Clubb RT. The structure of the excisionase (Xis) protein from conjugative transposon Tn916 provides insights into the regulation of heterobivalent tyrosine recombinases. J Mol Biol. 2005; 347:11–25. [PubMed: 15733914]
32. Sam MD, Cascio D, Johnson RC, Clubb RT. Crystal structure of the excisionase-DNA complex from bacteriophage lambda. J Mol Biol. 2004; 338:229–40. [PubMed: 15066428]
33. Zwieb C, Adhya S. Plasmid vectors for the analysis of protein-induced DNA bending. Methods Mol Biol. 2009; 543:547–62. [PubMed: 19378186]
34. Elantak L, Ansaldi M, Guerlesquin F, Mejean V, Morelli X. Structural and genetic analyses reveal a key role in prophage excision for the TorI response regulator inhibitor. J Biol Chem. 2005; 280:36802–8. [PubMed: 16079126]
35. Rice PA, Yang S, Mizuuchi K, Nash HA. Crystal structure of an IHF-DNA complex: a protein-induced DNA U-turn. Cell. 1996; 87:1295–306. [PubMed: 8980235]
36. Ball CA, Johnson RC. Efficient excision of phage lambda from the Escherichia coli chromosome requires the Fis protein. J Bacteriol. 1991; 173:4027–31. [PubMed: 1829453]
37. Ball CA, Johnson RC. Multiple effects of Fis on integration and the control of lysogeny in phage lambda. J Bacteriol. 1991; 173:4032–8. [PubMed: 1829454]
38. Lee MH, Pascopella L, Jacobs WR Jr. Hatfull GF. Site-specific integration of mycobacteriophage L5: integration-proficient vectors for Mycobacterium smegmatis, Mycobacterium tuberculosis, and bacille Calmette-Guerin. Proc Natl Acad Sci U S A. 1991; 88:3111–5. [PubMed: 1901654]
39. Studier FW. Protein production by auto-induction in high density shaking cultures. Protein Expr Purif. 2005; 41:207–34. [PubMed: 15915565]
40. Otwinowski Z, Minor W. Processing of X-ray Diffraction Data Collected in Oscillation Mode. Methods in Enzymology. 1997; 276:307–326.
41. Adams PD, Afonine PV, Bunkoczi G, Chen VB, Davis IW, Echols N, Headd JJ, Hung LW, Kapral GJ, Grosse-Kunstleve RW, McCoy AJ, Moriarty NW, Oeffner R, Read RJ, Richardson DC, Richardson JS, Terwilliger TC, Zwart PH. PHENIX: a comprehensive Python-based system for macromolecular structure solution. Acta Crystallogr D Biol Crystallogr. 2010; 66:213–21. [PubMed: 20124702]
42. Davis IW, Leaver-Fay A, Chen VB, Block JN, Kapral GJ, Wang X, Murray LW, Arendall WB 3rd, Snoeyink J, Richardson JS, Richardson DC. MolProbity: all-atom contacts and structure validation for proteins and nucleic acids. Nucleic Acids Res. 2007; 35:W375–83. [PubMed: 17452350]
43. Kim J, Zwieb C, Wu C, Adhya S. Bending of DNA by gene-regulatory proteins: construction and use of a DNA bending vector. Gene. 1989; 85:15–23. [PubMed: 2533576]

## Highlights

- Mycobacteriophage Pukovnik can support excision in the absence of mIHF.
- Helical Pukovnik Xis filaments contain canonical and domain-swapped protomers.
- Xis introduces a 106° bend in *attR* DNA consistent with the filament structure.
- The highly bent filament constrains intasome architecture to enforce directionality.

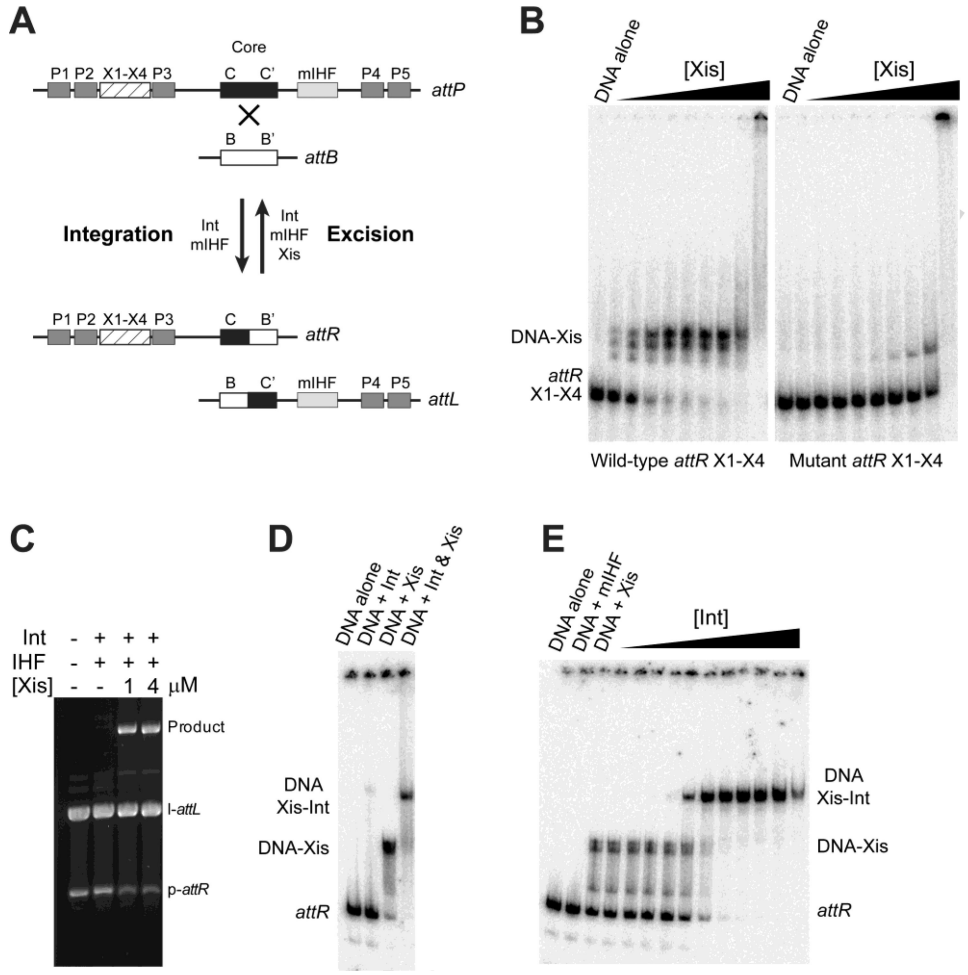


**Figure 1. Pukovnik Xis promotes integrase-mediated excisive recombination**

**A)** Organization of mycobacteriophage attachment sites. The phage and bacterial attachment sites, *attP* and *attB* respectively, each contain core-type integrase binding sites (C and C' in *attP*, B and B' in *attB*) flanking the sites of strand exchange; *attP* also contains arm-type integrase binding sites P1 – P5 (grey) and a region to which mycobacterial integration host (mIHF) is predicted to bind (light grey). Integrase (Int) mediates both integrative- and excisive-recombination, and both reactions typically require mIHF. Excision requires excise (Xis), which also inhibits integration. The Xis binding sequence is indicated with crosshatched box. B) Xis-DNA complexes were formed using a 50 bp *attR* fragment containing X1-X4 sites or an equivalent fragment with mutations within the X1-X4 sites, and separated using native gel electrophoresis. The Xis protein concentrations were 0, 0.125, 0.25, 0.5, 1, 2, 4, 8, 16, 32 μM. C) Pukovnik gp37 is a functional Xis. Int, mIHF, and Xis were mixed with linear *attL* (0.12 pmol) and plasmid *attR* (0.03 pmol) DNA substrates. The formation of a linear Product is separated on 0.8% agarose gel in 1x TBE running buffer and visualized by ethidium bromide staining. D) Xis promotes Int binding. Int (250 nM) and Xis (100 nM) were mixed with a 365 bp *attR* fragment as indicated and the resulting complexes separated by native gel electrophoresis. E) Xis but not IHF is required for *attR* intasome formation. Xis (100 nM), mIHF (25 nM) and Int were mixed with *attR* DNA and separated as in D. Int concentrations were 0, 0.3, 0.9, 2.7, 8.1, 24, 74, 220, 670, 2000, and 6000 nM.

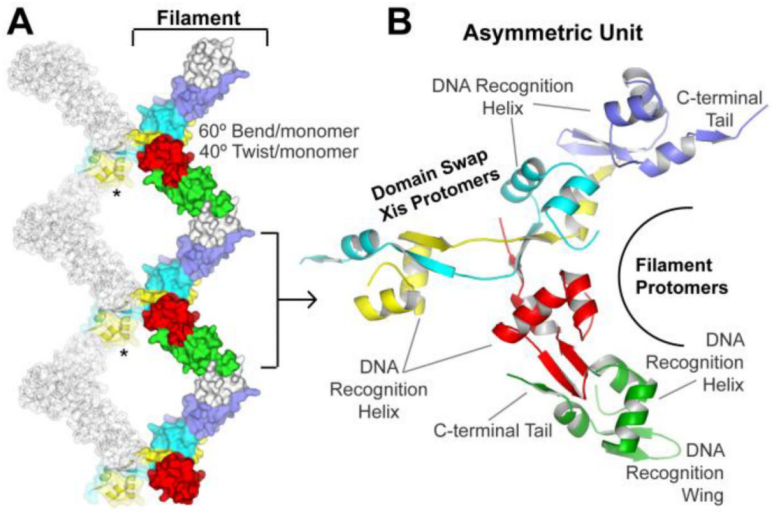


**Figure 2. Structure of Pukovnik Xis**

A) Xis protomer packing within the crystal forms left-handed superhelical filaments. Surface representation of Xis protomers (Green, Red, Blue, Yellow and Cyan) which pack together to form an Xis filament. Adjacent filaments are bridged by canonical packing of a domain swapped protomer (*), while the white protomer is a domain swapped Xis from an adjacent filament. B) Cartoon representation of the asymmetric unit. The positions of the four filament forming Xis protomers are indicated, as are the positions of the DNA recognition helices and the C-terminal tail which packs next to the wing, providing a platform for Xis-Xis interactions that drives cooperative DNA binding.

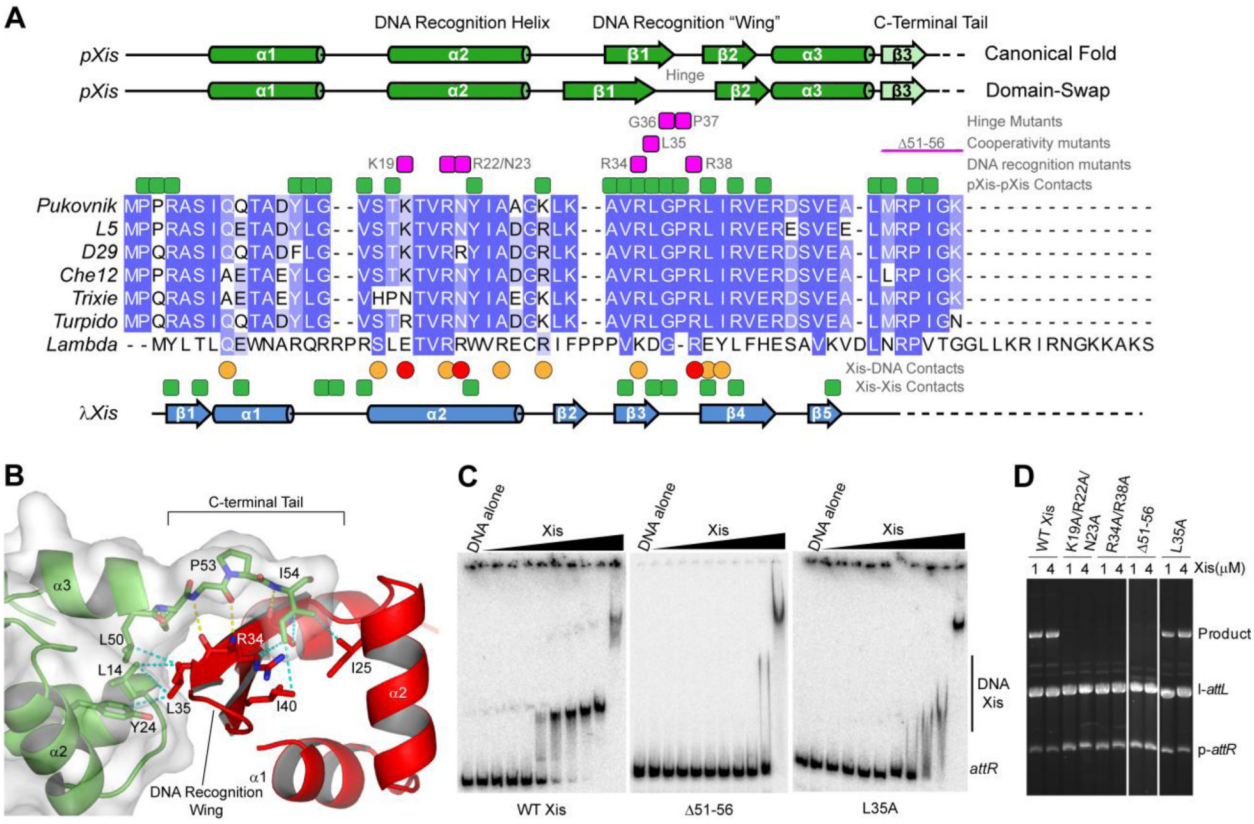


**Figure 3. Predicted DNA binding residues and observed Xis protomer contacts are both important for DNA binding and excision**

A) Observed secondary structure for Xis protomers with either the canonical or domain swapped fold. Multiple sequence alignment for related Xis proteins and lambda. Residues mediating Xis-Xis contacts in both Pukovnik and Lambda are indicated (green squares), as are the residues with base specific (red) and phosphate backbone (orange) DNA contacts. B) Xis-Xis contacts in Pukovnik Xis are formed by packing of the C-terminal tail against the DNA recognition Wing as well as a series of hydrophobic interactions centered around L35. C) Xis-DNA complexes were formed using a 365 bp *attR* fragment and the indicated Xis mutant predicted to impair Xis-Xis contacts. Complexes were separated using native gel electrophoresis. The Xis protein concentrations were 0, 1.6 nM, 4.8 nM, 14.6 nM, 43 nM, 131 nM, 390 nM, 1.2 μM, 3.5 μM, 10.6 μM, and 32 μM. D) DNA recognition residues and the C-terminal tail are each required for excision. The indicated Xis mutants were mixed with mIHF, Int, linear *attL* and plasmid *attR* as in Fig 1. Reaction products are separated using 0.8% agarose in 1X TBE running buffer and visualized using ethidium bromide staining.

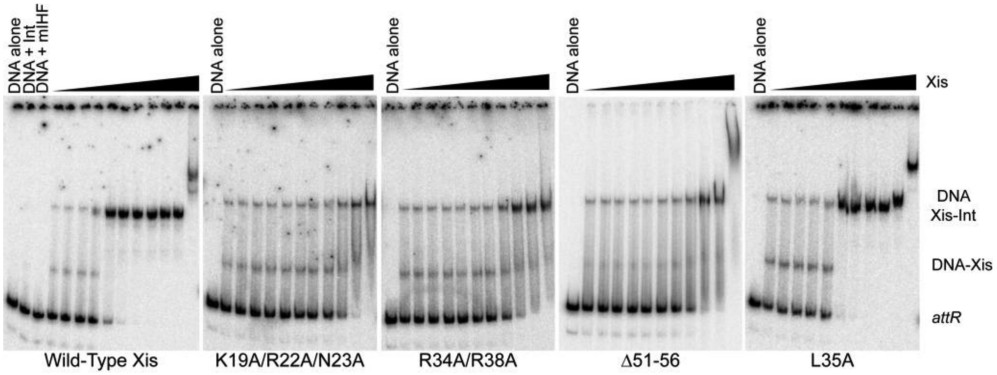


**Figure 4. DNA recognition and filament formation contribute to attR intasome assembly**

Int (100 nM) and mIHF (25 nM) were mixed with a 365 bp *attR* DNA fragment and the indicated Xis variant. The Xis protein concentrations were 0, 1.6 nM, 4.8 nM, 14.6 nM, 43 nM, 131 nM, 390 nM, 1.2 μM, 3.5 μM, 10.6 μM, and 32 μM. The formation of an *attR* intasome containing *attR*, Int, and Xis was monitored using native gel electrophoresis.

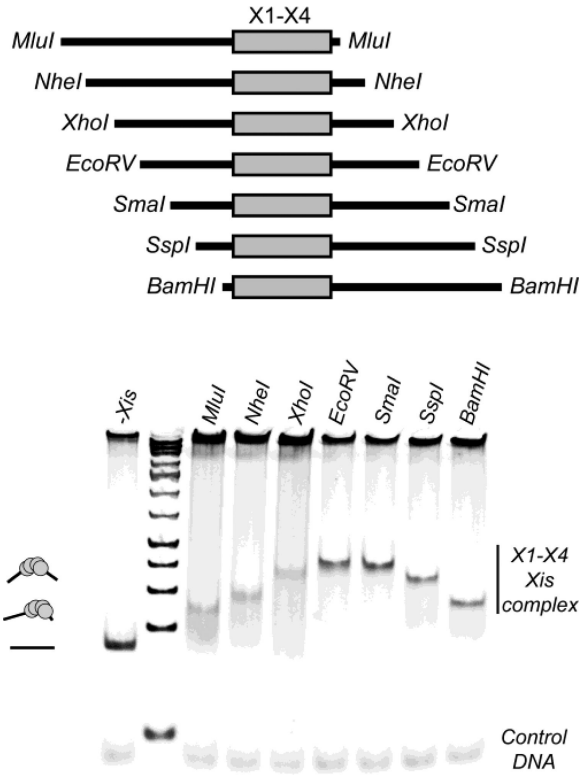


**Figure 5. Pukovnik Xis-mediated bending in X1-X4**

Top) Diagram of DNA binding substrates used in the permutation assay. Substrates are liberated from the pBEND2 plasmid via digestion with the indicated restriction enzyme and contain the same length of DNA with differentially positioned X1-X4 binding cassette. Bottom) Measuring Xis-mediated DNA bending *in vitro*. 25 ng of DNA substrates of equal length are liberated from the pBEND2 plasmid via digestion with the indicated restriction enzyme, mixed with 10 ng of an unrelated non-specific DNA control and Xis (2 μM) and complexes separated by native gel electrophoresis and detected by SybrGreen. Differential migration of the resulting complex was used to calculate the bending angle as described [33].

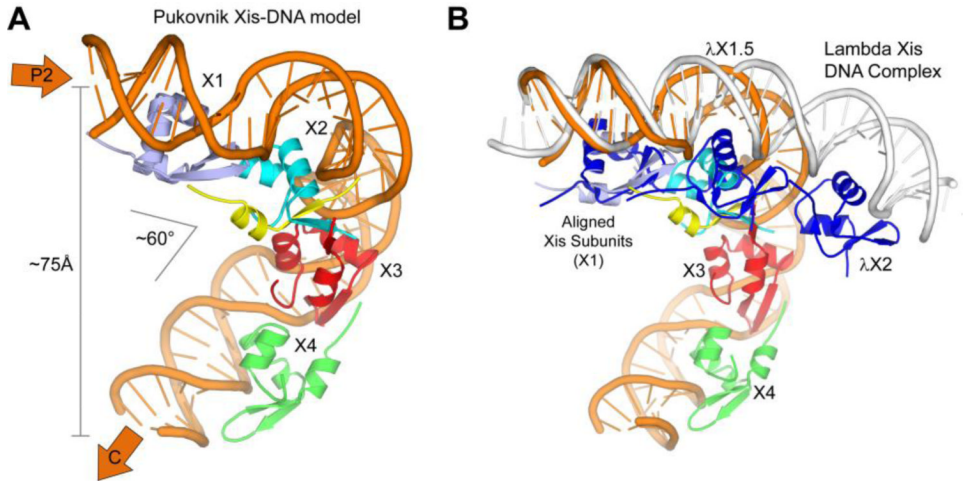


**Figure 6. Model of a Pukovnik Xis nucleofilament**

A) Insight into filament architecture. A model of Pukovnik Xis-DNA filament was constructed by removing the bridging domain-swapped Xis protomer to obtain a Pukovnik Xis protein filament to which DNA was added by superposition with the Lambda Xis-DNA complex (2IEF, Chain B and the DNA associated with chain B). Pukovnik Xis monomers are colored as in Figure 2, as is the direction of P2 and C DNA sequences within *attR*. B) The Pukovnik Xis-DNA model was structurally aligned to the Lambda Xis-DNA complex via the proximal Xis protomer (X1, PDB 2IEF, chain C). Lambda Xis proteins are colored dark blue and their positions X1, X1.5, and X2 indicated. DNA from the Lambda Xis-DNA complex is colored white, while DNA from the Pukovnik Xis-DNA model is colored orange.

## Table 1

Crystallographic Data collection and Refinement statistics

| | SeMet Xis | Native Xis |
|---|---|---|
| **Data collection** | | |
| Space group | C 2 2 $2_1$ | C 2 2 $2_1$ |
| Cell dimensions | | |
| *a, b, c* (Å) | 89.66, 130.67, 92.23 | 89.42, 129.99, 92.34 |
| Resolution (Å) | 90 - 2.30 (2.34-2.30) | 90 - 2.35 (2.39-2.35) |
| $R_{merge}$ | 0.092 (0.500) | 0.065 (0.697) |
| $I / \sigma I$ | 28.63 (2.17) | 22.72 (2.48) |
| Completeness (%) | 90.1 (58.1) | 99.77 (88.8) |
| Redundancy | 6.0 (5.3) | 5.8 (4.2) |
| **Refinement** | | |
| Resolution (Å) | | 36.86 - 2.35 (2.44-2.35) |
| Reflections | | 22,795 |
| $R_{work}$ / $R_{free}$ | | 0.2257 / 0.2670 |
| Number of. atoms | | |
| Protein | | 2121 |
| Ligand/ion | | 35 |
| Water | | 144 |
| B-factors | | |
| Protein | | 54.53 |
| Ligand/ion | | 75.54 |
| Water | | 55.85 |
| R.m.s. deviations | | |
| Bond lengths (Å) | | 0.007 |
| Bond angles (°) | | 0.984 |

*Values in parentheses are for highest-resolution shell.